Syntheses, Structures and Theoretical Investigations of $1\lambda^4,3\lambda^4,5\lambda^4$-Trithia-2,4,6,8,9-pentaazabicyclo[3.3.1]nona-1(9),2,3,5,7-pentaenes

Carsten Knapp,[a] Enno Lork,[a] Tobias Borrmann,[b] Wolf-Dieter Stohrer,[b] and Rüdiger Mews*[a]

Keywords: Sulfur / Nitrogen / Fluorine / Solid-state structures / Quantum chemistry

The syntheses of the title compounds RCN_5S_3 with electron-withdrawing aryl substituents [R = 2-FC_6H_4 (**1m**), 4-FC_6H_4 (**1n**), 2,6-$F_2C_6H_3$ (**1o**), C_6F_5 (**1p**), 4-NCC_6H_4 (**1q**) and Cl_3C (**1r**)] are described. The X-ray structures of **1n**, **1o**, **1q** and **1r**, together with those of $Me_2NCN_5S_3$ (**1b**) and 4-$CH_3C_6H_4CN_5S_3$ (**1f**), are reported. The experimentally determined dependence of the bond lengths on the substituents R within the bicyclic system RCN_5S_3 is well-reflected in the results of the theoretical calculations (RHF, MP2, B3LYP). The bonding model developed shows that acceptor substituents do not influence bonding within the bicycle. In the solid state, two fundamentally different primary interactions of the RCN_5S_3 molecules are observed; "stacking" and "dimerisation", which can be rationalised by electrostatic interactions between the CN_5S_3 units. However, secondary effects – the interactions between the R substituents – may be even more dominant.

Introduction

The bicyclic carbon-sulfur-nitrogen heterocycles, $1\lambda^4,3\lambda^4,5\lambda^4$-trithia-2,4,6,8,9-pentaazabicyclo[3.3.1]nona-1(9),2,3,5,7-pentaenes **1** (Scheme 1), are multifunctional sulfur-nitrogen systems with a versatile chemistry.

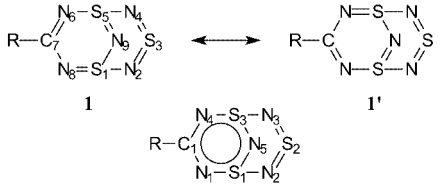

1 **1'**

R = X_3C [X = F (**1a**), Cl (**1r**)]
= R''_2N [R'' = Me (**1b**), Et (**1c**), *i*-Pr (**1d**)]
= $R'C_6H_4$ [R' = H (**1e**), 4-H_3C (**1f**), 4-Cl (**1g**), **4**-F_3C (**1h**), 4-H_3CO (**1i**), 4-C_6H_5 (**1j**), 3-F_3C (**1k**), 4-NC (**1q**)]
= Ar_F [Ar_F = 2-FC_6H_4 (**1m**), 4-FC_6H_4 (**1n**), 2,6-$F_2C_6H_3$ (**1o**), C_6F_5 (**1p**)]
= Cl (**1l**)

Scheme 1. Note: The numbering in the top left represents the IUPAC numbering scheme, the scheme below is that used consistently in this article

They are accessible via two different routes, either from the reaction of 1,3-dichloro-1,3-dithiatriazines $(RCN)(NSCl)_2$ with $Me_3SiNSNSiMe_3$ (dithiatriazine route A; Scheme 2), or from $(NSCl)_3$ and tris(trimethylsilyl)amidines $RC(NSiMe_3)[N(SiMe_3)_2]$ (amidine route B).

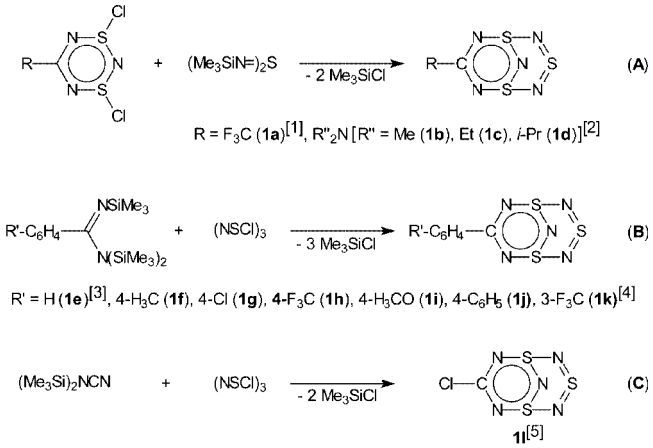

Scheme 2

The preparation of the chloro derivative, described by route C,[5] is difficult to reproduce, but the compound is also accessible via route A from $(ClCN)(NSCl)_2$.[6] Attempts to prepare the corresponding fluoro derivative from $(FCN)(NSCl)_2$ resulted in a very unstable product.[6]

[a] Institut für Anorganische und Physikalische Chemie der Universität Bremen,
Postfach 330440, Leobener Straße, 28334 Bremen, Germany
Fax: (internat.) +49-(0)421/218-4267
E-mail: mews@chemie.uni-bremen.de
[b] Institut für Organische Chemie der Universität Bremen,
Postfach 330440, Leobener Straße, 28334 Bremen, Germany
Supporting information for this article is available on the WWW under http://www.eurjic.org or from the author.

To date, the chemistry of these systems has not been well investigated. Based on MNDO calculations,[7] it has been proposed that the coordination chemistry of compounds **1** is varied. From the large number of chemically non-equivalent donor and acceptor sites in **1**, many interesting and not readily predictable reaction possibilities are expected. To date, only the F_3C derivative **1a** has been introduced as a ligand. $[Ni(F_3CCN_5S_3)_2(OSO)_2(FAsF_5)_2]$ and $[Ag(F_3CCN_5S_3)(\mu\text{-}F_3CCN_5S_3)]_2(AsF_6)_2$ have been isolated and characterised by X-ray crystallography.[7] The bicyclic system undergoes nucleophilic attack with EPh_3 (E = P, As), and **1e** is transformed into the monocyclic eight-membered imino derivatives **2** (Scheme 3),[8] with weak transannular S−S bonds.

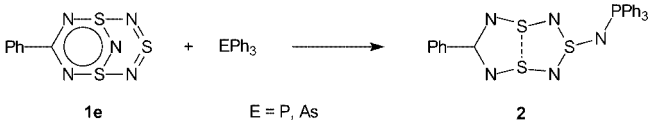

Scheme 3

Under the conditions of both thermolysis and photolysis,[9] it was recently found that the bicyclic sulfur-nitrogen heterocycles **1** afford the corresponding 1,2,3,5-dithiadiazolyl radicals, which are of high interest.[10]

The dependence of the reactivity on the substituent R is documented in the reaction of **1a** and **1e**−**k** with elemental chlorine. The aryl derivatives **1e**−**k** are readily degraded to dithiatriazines **3e**−**k** (Scheme 4),[3,4] while the trifluoromethyl derivative **1a** is not attacked under similar conditions.[11,12]

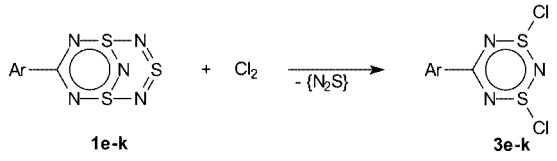

Scheme 4

From the structural and theoretical investigations we endeavoured to explain the different stabilities. Furthermore, these theoretical investigations should allow us to predict the reactivities and the properties of **1**, based on the nature of the substituent.

The X-ray structures of **1a**,[1] **1d**,[3,13] **1e**[14] and **1l**[5] have been described previously. A preliminary theoretical discussion of the bonding properties based on MNDO calculations was reported earlier by our group.[1] In this paper, the synthesis of compounds with electron-withdrawing substituents [RCN_5S_3: R = 2-FC_6H_4 (**1m**), 4-FC_6H_4 (**1n**), 2,6-$F_2C_6H_3$ (**1o**), C_6F_5 (**1p**), 4-NCC_6H_4 (**1q**) and Cl_3C (**1r**)], for which an increased stability is expected, are reported. The X-ray structures of selected compounds (**1b**, **1f**, **1n**, **1o**, **1q** and **1r**) have been determined. The experimental results are compared with the results of the theoretical calculations.

Results and Discussion

Syntheses of $1\lambda^4,3\lambda^4,5\lambda^4$-trithia-2,4,6,8,9-pentaazabicyclo-[3.3.1]nona-1(9),2,3,5,7-pentaenes

As expected, the bicyclic sulfur nitrogen systems **1m**−**1o** with partially fluorinated aryl substituents are readily prepared by the amidine route B from silylated amidines and trithiazyl trichloride. This route can also be used for the preparation of the trifluoromethyl-substituted derivative **1a** (Scheme 5). Thus, **1a** is more-readily accessible than previously reported.[1] It is not possible to use route B for the preparation of derivatives with stronger electron-withdrawing aryl groups (e.g. C_6F_5, 4-NCC_6H_4), since the corresponding *N*,*N*,*N*′-tris(trimethylsilyl)amidines cannot be prepared by silylation of lithium *N*,*N*′-bis(trimethylsilyl)amidines with Me_3SiCl. Their reactivity is greatly reduced due to the electron-withdrawing groups.[15,16] In this case, the corresponding lithium *N*,*N*′-bis(trimethylsilyl)amidines are directly reacted with $(NSCl)_3$ in diethyl ether. Under these conditions, **1p** and **1q** are also formed, but in lower yields. The compounds were obtained in a pure crystalline state by recrystallisation from acetonitrile.

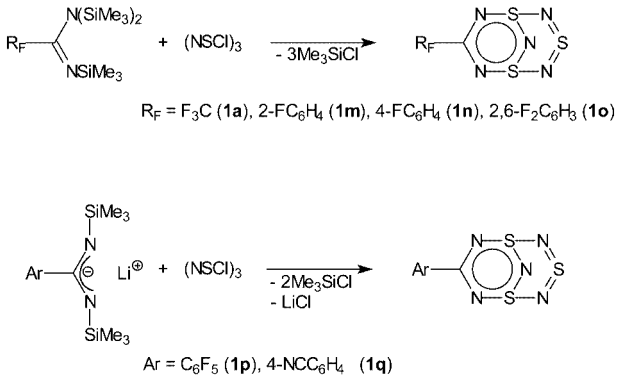

Scheme 5

Compounds **1** can be stored at room temperature in an inert atmosphere and do not decompose. The bicyclic sulfur nitrogen framework undergoes chemical, photochemical or thermal decomposition (partial or complete). In moist air, most of the bicycles are transformed into a white solid within a few hours or days. Even $PhCN_5S_3$, described in the literature as air-stable,[3] will slowly decompose under these conditions. Complete hydrolysis occurs according to Scheme 6:

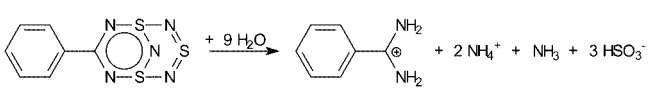

Scheme 6

The products from the direct complete hydrolysis in moist CH_2Cl_2, detected by mass spectrometry (FAB) and chemical analysis, are the corresponding amidinium ions and the NH_4^+, sulfate and thiosulfate ions; only small amounts of the sulfite ion are detected.

The results of the mass spectrometric analysis of the pure bicyclic systems depend on the ionisation method applied. With ionisation by EI, molecular ions are mostly detected, but with low intensity. The peak representing the fragment $[M - N_3S]^+$ is always present. This corresponds to the stable 1,2,3,5-dithiadiazolylium cation b^+ (Scheme 7) The more gentle FI method also allows for the detection of molecular ions. Furthermore, the direct degradation products a^+ and b^+ are observed, together with the ions (c^+, d^+) formed by recombination of the fragments.

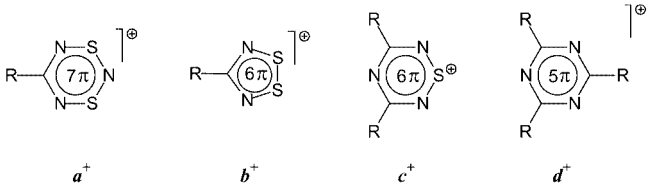

Scheme 7

Chlorine cleaves the NSN bridge of the aryl-substituted bicyclic systems, forming the 1,3-dichloro-1,3,2,4,6-dithiatriazines.[3,4] In contrast to the aryl derivatives, the trifluoromethyl derivative $F_3CCN_5S_3$ (**1a**) is astonishingly stable and does not react with elemental chlorine or with SO_2Cl_2.[4,11,12] Attempts to obtain the corresponding dithiatriazines by degradation reactions of **1a** with Br_2 or $(CF_3)_2NO$ also failed.[12] To date, no explanation for the unexpected stability could be given. In contrast to **1a**, the partially and fully fluorinated aryl derivatives **1o** and **1p** also react with chlorine in CCl_4 (the reaction occurs within a few minutes) to give the corresponding 1,3-dichloro-1,3,2,4,6-dithiatriazines. An obvious dependence of the rate of chlorination on the substituents at the aryl groups has been noted for electron-withdrawing groups (**1g**, **1h**) vs. electron-donating groups (**1f**, **1i**).[4]

Some years ago investigations on the thermal decomposition of $PhCN_5S_3$ (**1e**) in acetonitrile solution were undertaken; only benzonitrile and S_4N_4 were identified as the decomposition products.[17] More recent investigations of the thermolysis of **1e** in squalane by ESR spectroscopy have shown that the radicals b˙ and c˙ are formed as the decomposition products, in accord with the results of the mass spectrometric investigations mentioned before. Both radicals are known from the literature and can be prepared by straightforward methods.[18]

Structure Investigations

Single crystals of RCN_5S_3 [R = Me_2N (**1b**), 4-$CH_3C_6H_4$ (**1f**), 4-FC_6H_4 (**1n**), 2,6-$F_2C_6H_3$ (**1o**), 4-NCC_6H_4 (**1q**), and Cl_3C (**1r**)] were obtained by crystallisation from acetonitrile at −40 °C. They crystallise in the triclinic space group $P\bar{1}$ with the exception of $Cl_3CCN_5S_3$ (**1r**), which crystallises in the monoclinic space group $P2_1/n$ with one molecule of acetonitrile in the asymmetric unit. Crystal data and details of the structure determinations are given in Table 1. Figure 1 shows the structures and the numbering scheme of **1o** and **1q** as representative examples. In these bicycles, the different substituents only have a slight effect on the bond lengths. The C1−N1 bond lengths (131.8−135.3 pm), the N1−S1 bond lengths (158.3−164.0 pm) and the S1−N5 bond lengths (162.6−163.4 pm) lie in the range between that of single and double bonds, while the S1−N2 bonds (172.3−174.8 pm) might be considered as single bonds and the N2−S2 bonds (154.0−155.2 pm) as double bonds. In line with the mesomeric structures (Scheme 1), the bicyclic

Table 1. Crystal data and structure refinement data for **1b**, **1f**, **1n**, **1o**, **1q**, and **1r**

	1b	**1f**	**1n**	**1o**	**1q**	**1r**
Empirical formula	$C_3H_6N_6S_3$	$C_8H_7N_5S_3$	$C_7H_4FN_5S_3$	$C_7H_3F_2N_5S_3$	$C_8H_4N_6S_3$	$C_4H_3Cl_3N_6S_3$
Molecular mass	222.32	269.37	273.33	291.32	280.35	337.65
Crystal system	triclinic	triclinic	triclinic	triclinic	triclinic	monoclinic
Space group	$P\bar{1}$	$P\bar{1}$	$P\bar{1}$	$P\bar{1}$	$P\bar{1}$	$P2_1/n$
a, pm	625.90(10)	594.90(10)	594.7(2)	603.70(10)	476.60(10)	592.50(10)
b, pm	754.30(10)	736.90(10)	746.3(2)	770.90(10)	1082.9(5)	2916.5(3)
c, pm	916.2(2)	1294.1(2)	1172.4(3)	1147.80(10)	1159.3(4)	693.10(10)
α, deg	89.710(10)	78.850(10)	101.53(3)	91.460(10)	64.53(2)	90
β,deg	80.26(2)	84.540(10)	90.31(3)	90.350(10)	87.97(2)	92.500(10)
γ, deg	76.540(10)	73.640(10)	105.95(2)	107.000(10)	78.63(3)	90
V, nm³	0.41434(12)	0.53357(14)	0.4892(2)	0.51062(4)	0.5288(3)	1.1966(3)
Z	2	2	2	2	2	4
$D_{calcd.}$, Mg/m³	1.782	1.677	1.856	1.895	1.761	1.874
Crystal size	0.60 × 0.40 × 0.30	0.70 × 0.60 × 0.10	0.70 × 0.50 × 0.20	0.60 × 0.40 × 0.20	0.40 × 0.30 × 0.20	0.60 × 0.40 × 0.30
θ range	2.78−27.50	2.93−27.49	2.90−27.50	2.76−27.50	3.45−23.50	2.79−26.50
Reflections collected	2227	4994	4551	4704	2997	3394
Independent reflections	1715	2460	2247	2327	1494	2488
Absorption correction	−	−	−	−	DIFABS	−
Goodness-of-fit	1.079	1.074	1.117	1.103	1.044	1.062
Final *R* indices *R*1, *wR*2	0.0359, 0.1006	0.0267, 0.0749	0.0261, 0.0744	0.0262, 0.0726	0.0656, 0.1578	0.0490, 0.1213
R indices (all data)	0.0375, 0.1019	0.0285, 0.0768	0.0276, 0.0760	0.0280, 0.0739	0.1043, 0.1802	0.0735, 0.1307

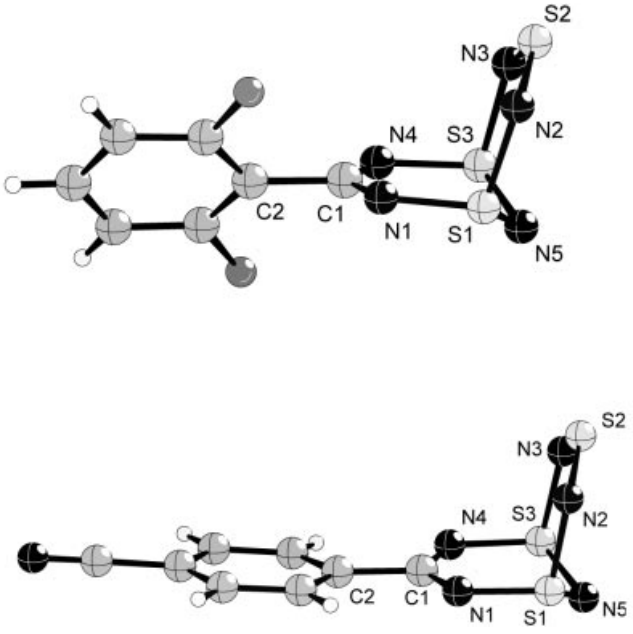

Figure 1. Crystal structures and numbering scheme of **1o** and **1q**

framework is best described as a dithiatriazine bridged by a sulfur diimide group.

Closer examination of the bonding parameters shows the effect of the substituents. The ten bicycles described in Table 2 can be divided into three groups. Strong donors or strong acceptors bonded directly to the bicycles each form one group. The third group consists of all aryl-substituted bicycles, the bond lengths of which are independent of the substituents at the aryl ring (they are equal within the range of standard deviations).

The difference between the three different groups is particularly apparent in the C1−N1 and the N1−S1 bond lengths. The C1−N1 bond length is increased by approximately 2 pm by electron-donating substituents (R = Me_2N), and shortened by approximately 1.5 pm by electron-accepting substituents (R = CF_3), relative to the weakly interacting phenyl group. The neighbouring N1−S1 bonds show the reverse effect. The effects on the other bonds in the system, except on the S1−N2 bond, are within experimental error. Directly bonded amino groups significantly increase this bond length when compared with the directly bonded electron-withdrawing groups and the aryl substituents.

The change in the C1−N1 bond lengths is accompanied by a change in the NCN angle: 127−128° for compounds with donor substituents, around 130° for the aryl derivatives, and up to 134−135° for the acceptor-substituted bicycles.

In the aryl derivatives the twist angle τ between the aromatic phenyl ring and the plane of the five atoms (C1, N1, N4, S1, S3) in the heterocycle is 26−29° for **1e**, **1f** and **1n**, i.e. the 6π-aromatic and the delocalised sulfur-nitrogen systems are not coplanar. However, in **1q**, which has a strongly electron-accepting nitrile group in the *para* position, the two rings are virtually coplanar (τ = 5.2°). However, this does not lead to an apparent shortening of the exocyclic C−C1 bond. In **1o**, the phenyl ring is 50.1° out of the plane formed by the five atoms of the heterocycle, because of the repulsive interactions between the fluorine atoms in the *ortho*-positions and the nitrogen atoms N1 and N4.

Solid-State Packing

In the crystal, the packing of the molecules varies. Two completely different arrangements of the bicycles are observed that can be described as "stacking" or "dimerisation". Stacking is found for the bicycles with R = Cl (**1l**), F_3C (**1a**) and 4-NCC_6H_4 (**1q**); a related structure is shown

Table 2. Selected bond lengths (pm) and angles (deg) for the bicyclic molecules RCN_5S_3

R	R−C1	C1−N1 C1−N4	N1−S1 N4−S3	S1−N5 S3−N5	S1−N2 S3−N3	N2−S2 N3−S2	NCN	τ	ref.
F_3C (**1a**)	152.4(4)	131.6(3) 132.5(3)	163.1(2) 163.0(2)	162.7(2) 163.3(2)	172.3(2) 172.7(2)	154.4(2) 154.6(2)	134.1(2)	–	[1]
Cl_3C (**1r**)	153.9(5)	131.6(5) 131.7(5)	163.7(3) 164.5(3)	162.9(4) 162.9(4)	172.6(3) 172.4(3)	154.1(3) 155.0(4)	133.9(4)	–	this work
Cl (**1l**)	175.1(2)	132.0(2) 131.9(2)	163.3(2) 163.2(2)	163.4(2)	173.1(2)	155.0(2)	135.2(3)	–	[5]
4-NCC_6H_4 (**1q**)	147.6(10)	132.5(9) 135.0(9)	162.0(6) 161.3(6)	163.0(6) 162.1(7)	173.9(7) 171.6(6)	152.5(7) 155.8(6)	129.2(7)	5.2	this work
2,6-$F_2C_6H_3$ (**1o**)	149.7(2)	133.3(2) 133.4(2)	162.76(14) 163.07(14)	163.37(14) 163.02(14)	172.97(16) 172.33(16)	155.02(15) 155.41(15)	131.91(15)	50.1	this work
4-FC_6H_4 (**1n**)	148.7(2)	133.8(2) 134.0(2)	162.39(14) 162.36(14)	163.15(14) 163.38(14)	173.49(16) 172.99(16)	155.09(15) 155.23(15)	133.35(15)	28.4	this work
C_6H_5 (**1e**)	148.5(3)	133.9(3) 133.3(3)	162.1(2) 162.1(2)	162.9(2) 163.0(2)	172.8(2) 172.8(2)	154.7(2) 154.6(2)	129.8(2)	26.6	[3,13]
4-$H_3CC_6H_4$ (**1f**)	148.82(19)	134.04(19) 134.17(18)	162.65(13) 162.62(13)	163.22(13) 163.52(13)	173.50(14) 173.23(15)	154.93(14) 155.32(14)	130.36(14)	27.2	this work
Me_2N (**1b**)	134.6(3)	135.2(3) 135.2(3)	159.69(18) 160.06(19)	163.51(19) 163.1(2)	175.45(19) 174.2(2)	154.66(19) 155.3(2)	128.67(19)	–	this work
iPr_2N (**1d**)	134.1(4)	135.0(5) 135.5(4)	158.8(3) 157.7(3)	163.3(3) 162.0(4)	174.5(3) 175.0(3)	153.6(3) 154.3(3)	127.0(3)	–	[2]

by (**1d**; R = *i*Pr$_2$N). The sulfur-nitrogen rings fit into one another like stacked crates. Most of the aryl-substituted bicycles [R = 4-H$_3$CC$_6$H$_4$ (**1f**), 4-FC$_6$H$_4$ (**1n**), 2,6-F$_2$C$_6$H$_3$ (**1o**)] and the dimethylamino derivative (**1b**) form centrosymmetric dimers. The structure of Cl$_3$CCN$_5$S$_3$ (**1r**), which crystallises with one equivalent of acetonitrile, is different and cannot be assigned to either of these two types.

The stacking of the bicycles is represented by **1q** in Figure 2. Each heterocycle has one $N^{\delta-}\cdots S^{\delta+}$ and one $N^{\delta-}\cdots C^{\delta+}$ interaction with the molecule above. The $N^{\delta-}\cdots S^{\delta+}$ interacting distance between the bridging nitrogen atom and the sulfur atom of the diimide bridge is around 300−310 pm (**1q** 299.2, **1l** 304.5, **1a** 311.8 pm), depending on the substituent at the bicycle, and thereby lies within the sum of the van der Waals radii (335 pm). The $N^{\delta-}\cdots S^{\delta+}$ distance in **1d** is significantly longer (327.4 pm), which can be attributed to the repulsive steric effect of the large isopropylamino groups. The same effect is also observed for the $N^{\delta-}\cdots C^{\delta+}$ distance between the bridging nitrogen atom and the carbon atom of the heterocycle. This distance is more than 100 pm longer for **1d** (438.8 pm) than for the other three bicycles (around 315 pm). This is barely within the sum of the van der Waals radii (320−325 pm). The average distance between the planes through the parallel phenyl rings is approximately 350 pm for **1q**.

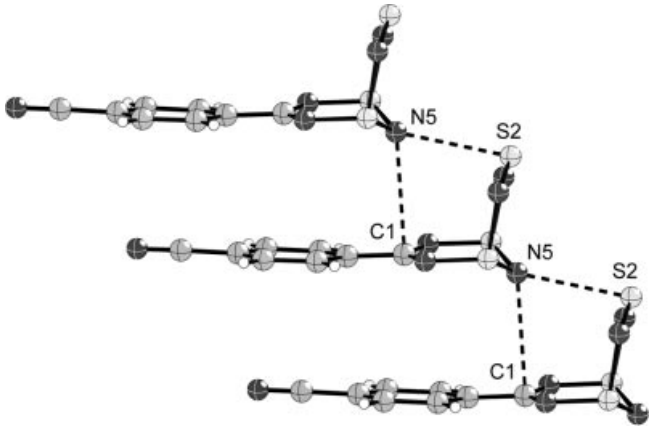

Figure 2. Stacking of **1q** in the crystal

In this case, "dimerisation" implies that two molecules are arranged with their heterocyclic heads facing each other (represented in Figure 3). The second molecule is rotated by 180° with respect to the first, so that two $N^{\delta-}\cdots S^{\delta+}$ interactions can be formed. The shortest distances between the molecules, independent of the substituent, is around 295 pm (**1o** 291.5−**11n** 296.4 pm), and is thus shorter than the sum of the van der Waals radii (335 pm).

Figures 4−6 present crystal packing diagrams that show the different arrangements of the bicycles in the crystal. Figure 4 shows details of the crystal lattice of **1q**, which is representative of the stacking arrangement. The structures of **1n** (Figure 5) and **1e** (Figure 6) show that the arrangement in the crystal is dependent on the substituents at the bicycles. The partially fluorinated aryl substituents form additional weak H-F interactions with neighbouring molecules. For example, in **1n** (Figure 5), this leads to a head-head/tail-tail arrangement of the molecules, thus forming a chain. The offset parallel chains form layers. In the phenyl derivative (**1e**), an arrangement (Figure 6) which resembles a fishbone pattern is observed.

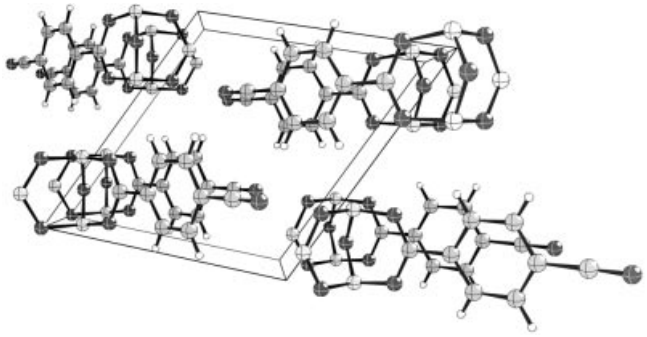

Figure 4. Crystal packing diagram of **1q**

Theoretical Calculations

Theoretical investigations were undertaken with the goal of finding explanations for the different stabilities of this bicyclic system with respect to the substituents, and for the different arrangements in the solid state. In Table 3, experimental bond lengths and bond angles for **1a** (R = CF$_3$), **1q** (R = 4-NCC$_6$H$_4$), **1e** (R = C$_6$H$_5$) and **1b** (R = Me$_2$N), representative examples for the different types of structures, are compared with the results of the RHF, MP2 and B3LYP calculations. As discussed previously, this bicyclic system is best described as a six-membered dithiatriazine with two sulfur atoms bridged by a sulfur diimide group. The experimental bond lengths within the dithiatriazine fragment are in reasonable agreement with all three methods, the best fit is found with the RHF calculations. The S1−N2 distances between the sulfur of the dithiatriazine fragment and the sulfur diimide group, obtained by the RHF method, are slightly shorter than those determined experimentally. The

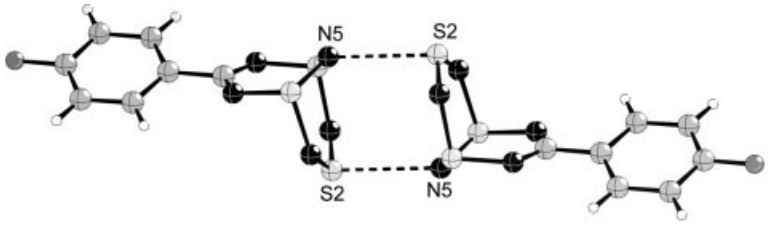

Figure 3. Centrosymmetric Dimer of **1n**

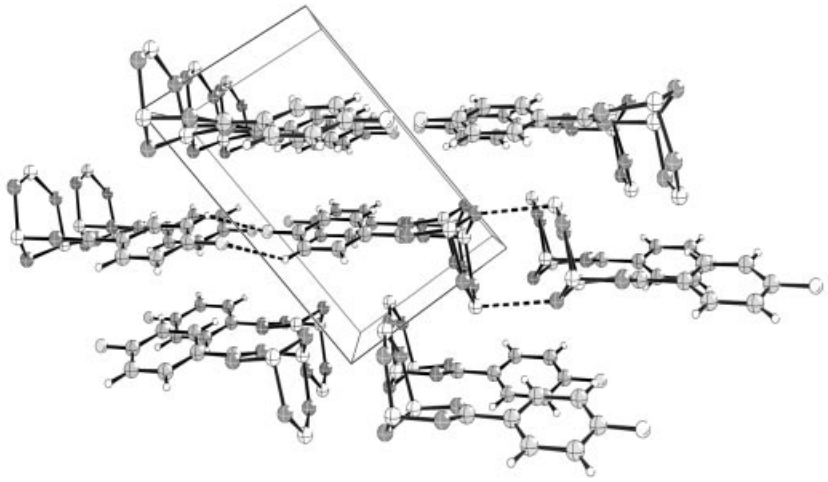

Figure 5. Crystal packing diagram of **1n**

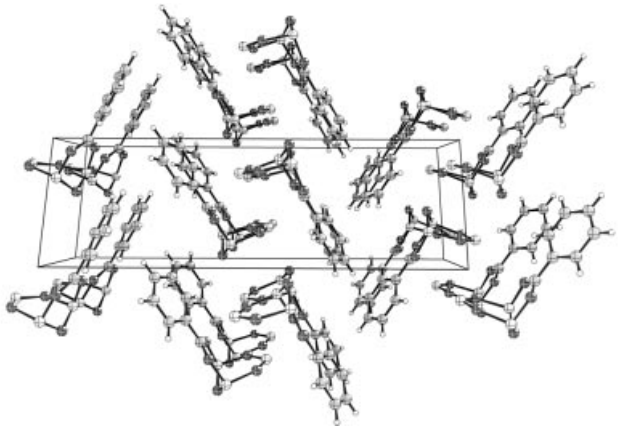

Figure 6. Crystal packing diagram of **1e**

distances resulting from the MP2 and B3LYP calculations are much larger. Similar results were obtained for the axial S−F distances in the related difluorodithiatriazines $RCN_3S_2F_2$ (R = F, CF_3). The RHF calculated distances are shorter and the MP2 and B3LYP calculated distances are much longer than those determined experimentally. The distances within the dithiatriazine are also well-reflected by all three methods.[19] The S2−N2 distances in the sulfurdiimide groups in **1**, calculated by the MP2 method, show the largest deviations (too long). Once again, the RHF calculated bond lengths are too short and those calculated by the B3LYP method are too long. Similar results have recently been obtained from the calculations of the molecular geometries of thioaminyl radicals.[20]

On the other hand, inspection of Table 3 shows that the experimentally determined influence of the different substituents on the bond lengths and on the NCN bond angle

Table 3. Averaged calculated (RHF/6−311G*, MP2/6−311G*, B3LYP/6−311G*) bond lengths and angles of **1a**, **1b**, **1e**, and **1q**

R	Method	C1−N1 (pm)	N1−S1 (pm)	S1−N5 (pm)	S1−N2 (pm)	N2−S2 (pm)	R−C1 (pm)	τ (deg)	N−C−N (deg)	NIMAG[a]
F_3C (**1a**)	Exp.	132.1	163.1	163.0	172.5	154.5	152.4(4)	−	134.1(2)	−
	RHF	130.5	162.4	161.2	170.8	151.3	153.2	−	133.3	0
	MP2	133.1	164.0	163.5	177.4	159.5	153.0	−	134.5	−
	B3LYP	132.4	165.4	165.3	178.7	156.9	154.2	−	133.8	0
H	RHF	131.3	162.4	161.5	171.1	151.3	−	−	133.0	0
	MP2	133.7	163.8	164.1	178.2	159.8	−	−	133.8	−
	B3LYP	133.0	165.5	165.8	179.1	157.0	−	−	133.8	0
4-NCC_6H_4 (**1q**)	Exp.	133.8	161.7	162.6	172.8	154.1	147.6(10)	5.2	129.2(7)	−
	RHF	131.9	161.5	161.2	171.3	151.2	149.7	0	130.0	0
	MP2	134.1	163.1	163.6	178.3	159.4	149.0	0	131.2	−
	B3LYP	133.8	164.2	165.3	179.5	156.8	149.4	0	130.3	0
C_6H_5 (**1e**)	Exp.	133.6	162.1	163.0	172.8	154.7	148.6(3)	26.6	129.8(2)	−
	RHF	132.2	161.1	161.3	171.6	151.2	149.2	0	129.5	0
	MP2	134.2	162.7	163.6	178.7	159.5	148.9	0	130.7	−
	B3LYP	134.1	163.8	165.5	180.1	156.8	149.0	0	129.7	0
Me_2N (**1b**)	Exp.	135.2	159.8	163.3	174.3	155.0	134.6(3)	−	128.67(19)	−
	RHF	133.6	159.6	161.4	172.1	151.2	134.3	−	128.5	0
	MP2	135.5	161.1	163.7	179.6	159.5	135.7	−	130.0	−
	B3LYP	135.4	162.0	165.6	180.9	156.8	135.9	−	128.7	0

[a] Number of imaginary frequencies.

is quite well-reflected by all three methods. Compared with the CF_3 derivative **1a**, C1−N1 increases by 1−1.5 pm in the aryl derivatives **1q**, **1e**, and to 2.5−3 pm in the Me_2N compound **1b**; S1−N1 decreases by 1−1.5 pm in **1q**, **1e** and to 2.8−3.4 pm in **1b**. S1−N5 and the diimide bond N2−S2 are not affected. According to the experiments, a marginal lengthening of the axial S1−N2 bond is observed when going from **1b** to **1q** and **1e**, the calculations show a slightly larger effect. A stronger influence on the lengthening of this bond is shown by experiment and by the calculations for **1b**, but this difference can hardly account for the different stabilities of **1q**, **1e**, **1b** compared with **1a**. The larger increase in the NCN angle in **1b** relative to **1q**, **1e** is also shown by experiment and by calculations.

The influence of the substituents can already be explained in terms of the (extended) frontier orbital model. The energetically highest occupied donor orbitals of the substituents interact with the energetically lowest unoccupied acceptor orbital of the bicycles with the same symmetry, as shown in Figure 7. By this, the *a priori* empty (unoccupied) acceptor orbital with antibonding character in the CN and bonding character in the SN region is partly populated, thus explaining the lengthening of the C−N and the shortening of the S−N bonds. These results are in perfect agreement with our MNDO calculations reported earlier.[1]

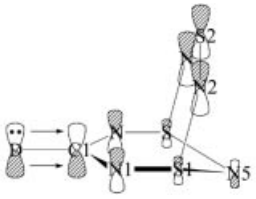

Figure 7. Interaction of the energetically highest occupied orbitals of the donor D with the energetically lowest unoccupied acceptor orbital with the same symmetry

Compared to the experimentally yet unknown hydrogen derivative included in the calculations in Table 3, acceptor substituents have no effect on the bond lengths. This is because the energetically highest occupied orbital in the bicycle with the appropriate symmetry is too low in energy for significant interaction with an empty acceptor orbital. The analysis of the orbitals with different model acceptors also confirms this. The acceptor orbital only shows negligible mixing with other orbitals. This also explains why the phenyl group acts as a donor only.

Another aim of the quantum chemical calculations was to find an explanation for the different crystallisation pattern: "stacking" and "dimerisation", and how this is dependent upon the substituents R.

The Mulliken and NBO charges (Table 4) for the atoms S2 and N5 at which the dimerisation occurs show virtually no dependency on the group R, therefore no correlation between the crystallisation pattern and the type of substituent can be observed. However, when we consider the MEP (mapped electrostatic potential),[21] which has also been utilised recently to rationalise the solid state packing of other SN systems,[22] a different picture is obtained. In Figure 8, representative examples for stacking (R = CF_3, Figure 8a) and dimerisation (R = NMe_2, Figure 8b) are shown. Positive electrostatic potential (ESP; blue) and negative ESP (red) fit perfectly together in the dimer of **1b** (R = NMe_2). For R = CF_3, the ESP's at S2 and N5 are not very pronounced. Furthermore, the negative potentials of N5 and C3 are lower than in the NMe_2 derivative, therefore "stacking" is less hindered by repulsive interactions.

Table 4. Calculated Mulliken and NBO charges (RHF/6−311G*) of **1a**, **1b**, **1e**, and **1q**

R	Method	C1	N1	S1	N5	N2	S2
F_3C (**1a**)	Mulliken	0.244	−0.608	0.998	−0.793	−0.710	1.006
	NBO	0.519	−0.899	1.546	−1.185	−1.070	1.466
4-NCC_6H_4 (**1q**)	Mulliken	0.555	−0.672	0.992	−0.793	−0.714	0.994
	NBO	0.626	−0.941	1.550	−1.189	−1.074	1.457
C_6H_5 (**1e**)	Mulliken	0.561	−0.672	0.985	−0.797	−0.716	0.985
	NBO	0.636	−0.947	1.547	−1.192	−1.072	1.450
Me_2N (**1b**)	Mulliken	0.737	−0.708	0.978	−0.807	−0.721	0.972
	NBO	0.821	−0.998	1.555	−1.199	−1.083	1.439

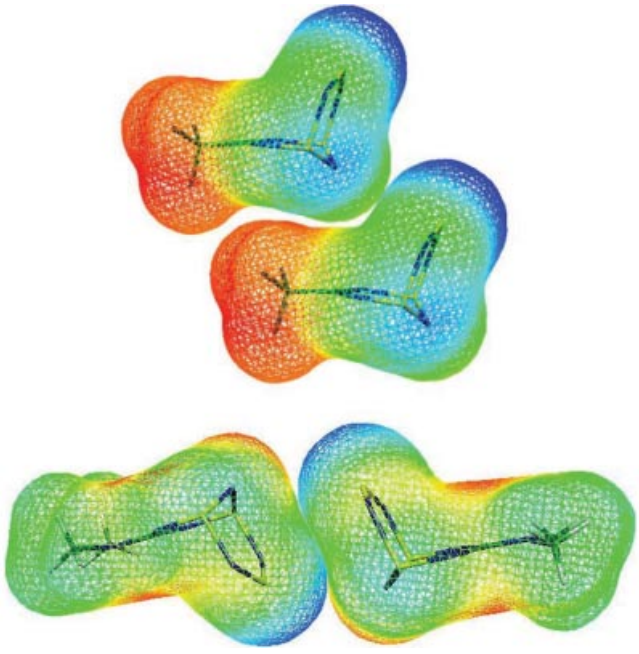

Figure 8. MEP (mapped electrostatic potential) of representative examples for stacking (R = CF_3) and for dimerisation (R = NMe_2)

Conclusions

Several new aryl 1λ⁴,3λ⁴,5λ⁴-trithia-2,4,6,8,9-pentaazabicyclo[3.3.1]nona-1(9),2,3,5,7-pentaenes RCN_5S_3 were prepared by the amidine route from $(NSCl)_3$ and $ArC(NSiMe_3)N(SiMe_3)_2$. When the persilylated amidines cannot be obtained from lithium-amidinates $RC(NSiMe_3)_2Li$ (R = C_6F_5, 4-NCC_6H_4) and Me_3SiCl, due to the decreased nucleophilicity of the amidinate, the amidinates can be used di-

rectly as starting materials. Contrary to our expectations, the introduction of electron-withdrawing aryl groups does not increase the stability of the RCN_5S_3 system.

The results of X-ray structure investigations and the theoretical calculations are in good agreement. The influence of the substituents on bonding is readily understood from the extended frontier orbital model. Compared with the parent hydrogen derivative, acceptor substituents have no effect, since the -CN_5S_3 HOMO of appropriate symmetry is too low in energy for significant interaction. The interaction of the donor orbitals with the LUMO of appropriate symmetry will increase the C−N bond lengths and decrease the lengths of the adjacent S−N bonds because the antibonding and bonding character in these regions is increased. The influence on the other bonds is only marginal because of the nonbonding character of the LUMO in these regions. The calculations show a slight increase of the S1−N2 bond lengths when going from electron-withdrawing to aryl to amino-substituted bicycles. The experimentally observed significant lengthening of the S1−N2 bond in the amino derivatives is not reflected by the calculations.

No explanation can be given for the unusual stability of the CF_3 derivative from the structural data and the theoretical calculations (the chemistry of the CCl_3 derivative was not investigated). From the large negative charges at the nitrogen centres (Table 4), the RCN_5S_3 derivatives are expected to act as multifunctional donor ligands. When going from CF_3 to aryl to Me_2N, only the positive charges at C1 and the negative charges at N2 increase, the charges at the other centres are not affected. Therefore, *a priori* the ligand properties should not be dependent on the substituents R.

In the solid state, two fundamentally different packing patterns are observed for RCN_5S_3, stacking of the RCN_5S_3 molecules and face-to-face dimerisation of the N_3S_3 subunits of the $-CN_5S_3$ bicycle. The dependence of the packing pattern on the substituents is difficult to predict. Primary electrostatic interactions are responsible for the different packing as shown by the MEP in Figure 8, but they might be dominated by steric requirements of the substituents R and by interactions between the substituents.

Experimental Section

Materials and Methods: All manipulations of air-sensitive materials were performed under an inert atmosphere of dry nitrogen, with the absence of oxygen and moisture. The fluorinated *N,N,N′*-tris-(trimethylsilyl)amidines {R = F_3C,[15] R = 4-FC_6H_4, 2-FC_6H_4, 2,6-$F_2C_6H_3$[16]}, $[(C_6F_5C(NSiMe_3)_2Li]_2{\cdot}OEt_2$,[16] $[(Me_3Si)_2NLi{\cdot}OEt_2]_2$,[23] $Cl_3CCN(NSCl)_2$,[24] $Me_3SiNSNSiMe_3$,[25] RCN_5S_3 [R = 4-$H_3CC_6H_4$, 4-$C_6H_5C_6H_4$,[4] R = Me_2N[2]] and trithiazyltrichloride $(NSCl)_3$[26] were prepared according to published procedures. Terephthalonitrile is a commercial compound. The solvents were carefully dried and distilled prior to use. NMR spectra were recorded on Bruker DPX 200 (^1H, ^{19}F) and on Bruker AM 360 NB (^{13}C) spectrometers in [D_1]chloroform. Chemical shifts are given with respect to Me_4Si. Infrared analyses were acquired as thin Kel-F and Nujol films (with KBr cells), using a Perkin−Elmer Paragon 500 FT-IR instrument. Mass spectra were measured on a Finnigan MAT 8200, using the field ionisation (FI) technique. The high-resolution mass spectra were obtained by using the peak matching method (chemical ionisation neg.). Melting points were obtained on a Gallenkamp melting point apparatus and are uncorrected.

Preparation of $F_3CCN_5S_3$ (1a): $F_3CC(NSiMe_3)[N(SiMe_3)_2]$ (13.7 g, 42 mmol) in 50 mL of dichloromethane was added dropwise to trithiazyl trichloride (10.0 g, 41 mmol) in 100 mL of dichloromethane at 0 °C. The solution became dark red. The solvent and all volatile products were removed and the remaining residue was dissolved in 100 mL of acetonitrile and the solution was filtered. On storage at −40 °C, yellow crystals were obtained (6.35 g, 26 mmol, 63% yield). The spectroscopic data are in accordance with literature data.[1] MS-FI: *m/z* = 247 (100) [M^+]. MS-HR: found 246.92615, calcd. 246.92679.

Preparation of 2-$FC_6H_4CN_5S_3$ (1m): 2-$FC_6H_4C(NSiMe_3)[N(SiMe_3)_2]$ (14.5 g, 41 mmol) in 100 mL of acetonitrile was added dropwise to trithiazyl trichloride (10.0 g, 41 mmol) in 100 mL of acetonitrile. The solution became dark red and a precipitate formed. The solvent and all volatile products were removed and the remaining residue was dissolved in 150 mL of boiling acetonitrile and the solution was filtered. On cooling to room temperature, yellow crystals were obtained (7.7 g, 28 mmol, 69% yield), m.p. 111 °C. ^1H NMR: δ = −7.16 ppm (ddd, $^3J_{H,F}$ = 11.3, $^3J_{H,H}$ = 8.3, $^4J_{H,H}$ = 1.0 Hz, 1 H, *m*-C_6H_4F), 7.25 (td, $^3J_{H,H}$ = 7.5, $^4J_{H,H}$ = 1.0 Hz, 1 H, *m*-C_6H_4F), 7.50 (dddd, $^3J_{H,H}$ = 8.3, $^3J_{H,H}$ = 7.5, $^4J_{H,F}$ = 4.8, $^4J_{H,H}$ = 2.0 Hz, 1 H, *p*-C_6H_4F), 7.91 (td, $^3J_{H,H}$ = 7.5, $^4J_{H,F}$ = 7.5, $^4J_{H,H}$ = 2.0 Hz, 1 H, *o*-C_6H_4F ppm. $^{13}C\{^1H\}$ NMR: δ = 117.1 (d, $^2J_{C,F}$ = 22 Hz, *m*-C_6H_4F), 124.1 (s, *m*-C_6H_4F), 125.4 (d, $^2J_{C,F}$ = 8 Hz, *ipso*-C_6H_4F), 130.8 (s, *o*-C_6H_4F), 133.6 (d, $^3J_{C,F}$ = 8 Hz, *p*-C_6H_4F), 161.1 (d, $^1J_{C,F}$ = 259 Hz, *o*-C_6H_4F), 165.6 (d, $^3J_{C,F}$ = 4 Hz, NCN) ppm. ^{19}F NMR: δ = −113.3 (ddd, $^3J_{F,H}$ = 11.3, $^4J_{F,H}$ = 7.5, $J_{F,H}$ = 4.8, 1F) ppm. IR: $\tilde{\nu}$ = 1508 w, 1485 m, 1451 m, 1410 m, 1342 s, 1263 w, 1226 m, 1154 m, 1101 m, 996 s, 927 m, 843 w, 822 w, 770 s, 745 s, 721 s, 685 w, 670 m, 574 s, 551 m, 504 s, 476 m cm^{-1}. MS-FI: *m/z* = 273 (48) [M^+]. MS-HR: found 272.96192, calcd. 272.96130.

Preparation of 4-$FC_6H_4CN_5S_3$ (1n): The procedure follows that of **1m**. 4-$FC_6H_4C(NSiMe_3)[N(SiMe_3)_2]$ (14.5 g, 41 mmol) was reacted with trithiazyl trichloride (10.0 g, 41 mmol). After recrystallisation from CH_3CN, **1n** (7.8 g, 29 mmol, 71% yield) was obtained as orange crystals, m.p. 132 °C. ^1H NMR: δ = 7.07−7.19 (m, 2 H, C_6H_4F), 8.18−8.28 (m, 2 H, C_6H_4F) ppm. $^{13}C\{^1H\}$ NMR: δ = 115.5 (d, $^2J_{C,F}$ = 21 Hz, *m*-C_6H_4F), 129.9 (d, $^3J_{C,F}$ = 9 Hz, *o*-C_6H_4F), 132.4 (d, $^4J_{C,F}$ = 2 Hz, *ipso*-C_6H_4F), 164.6 (s, NCN), 166.1 (d, $^1J_{C,F}$ = 237 Hz, *p*-C_6H_4F) ppm. ^{19}F NMR: δ = −107.2 (tt, $^3J_{F,H}$ = 8.3, $^4J_{F,H}$ = 5.5 Hz, 1F) ppm. IR: $\tilde{\nu}$ = 2932 w, 1594 m, 1503 m, 1422 s, 1360 m, 1339 s, 1296 w, 1225 m, 1152 m, 1093 w, 997 s, 967 sh, 926 w, 849 m, 829 w, 814 m, 776 s, 750 s, 718 s, 688 w, 668 m, 629 w, 597 w, 573 s, 516 w, 490 s, 480 m cm^{-1}. MS-FI: *m/z* = 273 (100) [M^+]. MS-HR: found 272.96244, calcd. 272.96130.

Preparation of 2,6-$F_2C_6H_3CN_5S_3$ (1o): 2,6-$F_2C_6H_3C(NSiMe_3)[N(SiMe_3)_2]$ (9.3 g, 25 mmol) was reacted with trithiazyl trichloride (6.1 g, 25 mmol). After recrystallisation from boiling acetonitrile and storage at −40 °C, **1o** (4.9 g, 17 mmol, 68% yield) was obtained as yellow-brown crystals, m.p. 104 °C. ^1H NMR: δ = 6.92−7.04 (m, 2 H, *m*-$C_6F_2H_3$), 7.32−7.43 (m, 1 H, *p*-$C_6F_2H_3$) ppm. $^{13}C\{^1H\}$ NMR: δ = 111.9 (dd, $^2J_{C,F}$ = 23, $^4J_{C,F}$ = 2 Hz, *m*-$C_6F_2H_3$), 111.9 (t, $^2J_{C,F}$ = 13 Hz, *ipso*-$C_6F_2H_3$), 131.8 (t, $^3J_{C,F}$ = 10 Hz, *p*-$C_6F_2H_3$), 159.8 (dd, $^1J_{C,F}$ = 254, $^3J_{C,F}$ = 6 Hz, *o*-$C_6F_2H_3$), 163.5

(s, NCN) ppm. ^{19}F NMR: δ = −114.9 (dd, $^3J_{F,H}$ = 7.8, $^4J_{F,H}$ = 6.2 Hz, 2F) ppm. IR: ṽ = 2926 w, 1622 m, 1591 m, 1566 w, 1472 m, 1344 s, 1238 m, 1148 m, 1011 s, 966 sh, 929 w, 818 w, 792 m, 776 m, 752 s, 630 m, 690 w, 670 m, 576 s, 523 w, 503 sh, 489 s, 467 m cm^{-1}. MS-FI: *m/z* = 291 (45) [M$^+$]. MS-HR: found 290.95194, calcd. 290.95187.

Preparation of $C_6F_5CN_5S_3$ (1p): $[C_6F_5C(NSiMe_3)_2Li]_2{\cdot}OEt_2$ (7.1 g, 18 mmol) in 50 mL of diethyl ether was added dropwise to trithiazyl trichloride (4.6 g, 19 mmol) in 50 mL of diethyl ether. The solution became dark red. The solvent and all volatile products were removed and the remaining residue was dissolved in 100 mL of acetonitrile and the solution was filtered. On storage at −40 °C, yellow-brown crystals were obtained (2.4 g, 7 mmol, 39% yield), m.p. 97 °C. ^{13}C{^{1}H} NMR: δ = 115.0 (t, $^2J_{C,F}$ = 17 Hz, *ipso*-C_6F_5), 138.7 (dm, $^1J_{C,F}$ = 253 Hz, *o*-C_6F_5), 143.2 (dm, $^1J_{C,F}$ = 253 Hz, *p*-C_6F_5), 145.2 (dm, $^1J_{C,F}$ = 247 Hz, *m*-C_6F_5), 162.1 (s, NCN) ppm. ^{19}F NMR: δ = −145.5 (dddd, $^3J_{FF}$ = −21.8, $^4J_{FF}$ = −4.7, $^4J_{FF}$ = 3.2, $^5J_{FF}$ = 8.0 Hz, 2F, *o*-F), −154.9 (tt, $^3J_{FF}$ = −20.2, $^4J_{FF}$ = 3.2, 1F, *p*-F), −164.3 (dddd, $^3J_{FF}$ = −21.8, $^3J_{FF}$ = −20.2, $^4J_{FF}$ = −0.8, $^5J_{FF}$ = 8.0 Hz, 2F, *m*-F) ppm. IR: ṽ = 1656 w, 1524 m,. 1504 s, 1427 sh, 1402 s, 1360 s, 1278 m, 1200 s, 1171 m, 1151 m, 1126 s, 1040 w, 1016 w, 986 m, 972 s, 901 m, 812 m, 761 sh, 722 s, 703 sh, 656 w, 626 w, 598 w, 570 w, 555 w, 531 m, 504 m, 473 m cm^{-1}. MS-FI: *m/z* = 345 (26) [M$^+$]. MS-HR: found 344.92149, calcd. 344.92361.

Preparation of 4-$NCC_6H_4CN_5S_3$ (1q): A solution of lithium bis(trimethylsilyl)amide (3.9 g, 16 mmol) and terephthalonitrile (2.1 g, 16 mmol) in 150 mL of diethyl ether was added dropwise to trithiazyl trichloride (4.4 g) in 50 mL of diethyl ether at 0 °C. The solution became brown. The solvent and all volatile products were removed and the remaining residue was dissolved in 100 mL of dichloromethane and the solution was filtered. On storage at −40 °C, orange crystals were obtained (1.4 g, 5 mmol, 31% yield), m.p. 158 °C. ^{1}H NMR: δ = 7.75 (ddd, $^3J_{H,H}$ = 8.3, $^4J_{H,H}$ = 2.0, $^5J_{H,H}$ = 1.5 Hz, 2 H, C_6H_4), 8.33 (ddd,$^3J_{H,H}$ = 8.3, $^4J_{H,H}$ = 2.0, $^5J_{H,H}$ = 1.5 Hz, 2 H, C_6H_4) ppm. ^{13}C{^{1}H} NMR: δ = 116.9 (s, *p*-C_6H_4), 119.0 (s, NC), 128.9 (s, *o*-C_6H_4), 133.0 (s, *m*-C_6H_4), 141.2 (s, *ipso*-C_6H_4), 165.4 (s, NCN) ppm. IR: ṽ = 2226 m, 1413 m, 1366 m, 1334 m, 1299 m, 1188 w, 1148 m, 1110 w, 1035 w, 1009 sh, 975 s, 921 w, 858 m, 836 w, 785 w, 768 sh, 750 m, 722 s, 692 m, 666 s, 642 sh, 561 m, 541 s, 506 m, 490 w, 467 m cm^{-1}. MS-FI: *m/z* = 280 (12) [M$^+$], 206 ($NCC_6H_4CN_2S_2^+$, 100). MS-HR: found 279.96632, calcd. 279.96597.

Preparation of $Cl_3CCN_5S_3$ (1r): $Me_3SiNSNSiMe_3$ (0.8 mL, 0.7 g, 3.5 mmol) in 10 mL of carbon tetrachloride was added dropwise to $Cl_3CCN(NSCl)_2$ (0.85 g, 2.7 mmol) in 25 mL of carbon tetrachloride. After standing overnight, the solvent and all volatile products were removed and the remaining residue was dissolved in a small amount of acetonitrile and the solution was filtered. On storage at −40 °C and after drying under vacuum, yellow crystals of **1r**·CH_3CN (0.55 g, 1.9 mmol, 68% yield) were obtained, m.p. 102 °C. ^{13}C NMR: δ = 97.3 (s, CCl_3), 168.4 (s, NCN) ppm. IR: ṽ = 1545 w, 1503 w, 1467 w, 1430 s, 1400 sh, 1362 m, 1292 s, 1265 sh, 1211 sh, 1202 m, 1171 w, 1151 m, 1127 w, 1028 m, 1004 sh, 987 m, 972 m, 946 sh, 916 sh, 872 sh, 862 m, 801 m, 758 m, 739 sh, 722 s, 702 w, 692 m, 660 m, 639 w, 567 m, 559 m, 506 s, 402 m cm^{-1}. MS-FI: *m/z* = 295 (58) [M$^+$]. MS-HR: found 294.83877, calcd. 294.83813.

Crystallographic Analysis

The single-crystal X-ray structure determinations were performed on a Siemens P4 diffractometer using Mo-K_α (0.71073 Å) radiation with a graphite monochromator. The crystals were mounted using Kel-F oil onto a thin glass fibre. Details of the data collection and refinement are given in Table 1. The programs SHELX-97[27] and DIAMOND[28] were used. The structures were solved by direct methods (SHELXS).[27] Subsequent least-squares refinement (SHELXL 97−2)[27] located the positions of the remaining atoms in the electron density maps. Non-hydrogen atoms were refined anisotropically. Hydrogen atoms were placed in calculated positions using a riding model and refined isotropically in blocks.

CCDC-205700 (**1b**) -205701 (**1f**) -205702 (**1n**) -205703 (**1r**) -205704 (**1o**) and -205705 (**1q**) contain the supplementary crystallographic data for this paper. These data can be obtained free of charge at www.ccdc.cam.ac.uk/conts/retrieving.html [or from the Cambridge Crystallographic Data Centre, 12, Union Road, Cambridge CB2 1EZ, UK; Fax: (internat.) +44-1223/336-033; E-mail: deposit@ccdc.cam.ac.uk].

Quantum Chemical Calculations: All *ab initio* calculations were performed with the GAUSSIAN′98 program package.[29] The mapped electrostatic potential (MEP) representations are made with MOLEKEL.[21]

Acknowledgments

Financial Support by the FNK, Universität Bremen is gratefully acknowledged.

[1] R. Maggiulli, R. Mews, W.-D. Stohrer, M. Noltemeyer, G. M. Sheldrick, *Chem. Ber.* **1988**, *121*, 1881−1889.
[2] T. Chivers, J. F. Richardson, N. R. M. Smith, *Inorg. Chem.* **1986**, *25*, 272−275.
[3] [3a] R. T. Boeré, A. W. Cordes, R. T. Oakley, *J. Chem. Soc., Chem. Commun.* **1985**, 929−930. [3b] R. T. Boeré, A. W. Cordes, R. T. Oakley, *Acta Crystallogr., Sect. C* **1985**, *42*, 1833−1834.
[4] R. T. Boeré, J. Fait, K. Larsen, J. Yip, *Inorg. Chem.* **1992**, *31*, 1417−1423.
[5] A. J. Banister, W. Clegg, I. B. Gorrell, Z. V. Hauptmann, R. W. H. Small, *J. Chem. Soc., Chem. Commun.* **1987**, 1611−1613.
[6] S. J. Chen, *Doctoral thesis*, Universität Bremen, Germany, **1993**.
[7] R. Maggiulli, R. Mews, W.-D. Stohrer, M. Noltemeyer, *Chem. Ber.* **1990**, *123*, 29−34.
[8] [8a] R. T. Boeré, A. W. Cordes, S. L. Craig, J. B. Graham, R. T. Oakley, J. A. J. Privett, *Chem. Commun.* **1986**, 807−808. [8b] R. T. Boeré, G. Ferguson, R. T. Oakley, *Acta Crystallogr., Sect. C* **1986**, *42*, 900−902. [8c] R. T. Boeré, A. W. Cordes, R. T. Oakley, *J. Am. Chem. Soc.* **1987**, *109*, 7781−7785.
[9] V. A. Bagryansky, N. P. Gritsan, Y. N. Molin, K. V. Shuvaev, A. V. Zibarev, personal communication.
[10] [10a] J. M. Rawson, A. J. Banister, I. Lavender, *Adv. Heterocyclic Chem.* **1995**, *62*, 137−247. [10b] J. M. Rawson, F. Palacio, *Struct. Bonding* **2001**, *100*, 93−128.
[11] R. T. Boeré, R. T. Oakley, R. W. Reed, N. P. C. Westwood, *Centenary of the Discovery of Fluorine, International Symposium*, Paris, **1986**, Abstr. I32.
[12] R. Maggiulli, *Diploma thesis*, Universität Göttingen, Germany **1986**.
[13] A. W. Cordes, R. T. Oakley, R. T. Boeré, *Acta Crstallogr., Sect. C* **1985**, *41*, 1833−1834.
[14] T. Chivers, F. Edelmann, J. F. Richardson, N. R. M. Smith, O. Treu Jr., M. Trsic, *Inorg. Chem.* **1986**, *25*, 2119−2125.
[15] R. T. Boeré, R. T. Oakley, R. W. Reed, *J. Organomet. Chem.* **1987**, *331*, 161−167.
[16] C. Knapp, E. Lork, P. G. Watson, R. Mews, *Inorg. Chem.* **2002**, *41*, 2014−2025.
[17] [17a] R. T. Boeré, R. T. Oakley, M. Shevalier, *J. Chem. Soc., Chem. Commun.* **1987**, 110−112. [17b] K. T. Bestari, R. T.

Boeré, R. T. Oakley, *J. Am. Chem. Soc.* **1989**, *111*, 1579−1584.
[18] [18a] P. J. Hayes, R. T. Oakley, A. W. Cordes, W. T. Pennington, *J. Am. Chem. Soc.* **1985**, *107*, 1346−1351. [18b] R. T. Boeré, R. T. Oakley, R. W. Reed, N. P. C. Westwood, *J. Am. Chem. Soc.* **1989**, *111*, 1180−1185.
[19] T. Borrmann, unpublished results
[20] P. Kaszynski, *J. Phys. Chem. A* **2001**, *105*, 7615−7625.
[21] Centro Svizzero di Calcolo Scientifico (CSCS), Manno, Switzerland.
[22] e.g. [22a] T. Borrmann, A. V. Zibarev, E. Lork, G. Knitter, S.-J. Chen, P. G. Watson, E. Cutin, M. M. Shakirov, W.-D. Stohrer, R. Mews, *Inorg. Chem.* **2000**, *39*, 3999− 4005. [22b] A. D. Bond, D. A. Haynes, C. M. Pask, J. M. Rawson, *J. Chem. Soc., Dalton Trans.* **2002**, 2522− 2531; A. D. Bond, D. A. Haynes, J. M. Rawson, *Can. J. Chem.* **2002**, *80*, 1507- 1517.
[23] M. F. Lappert, M. J. Slade, A. Singh, J. L. Atwood, R. D. Rogers, R. Shakir, *J. Am. Chem. Soc.* **1983**, *105*, 302−304.
[24] A. Apblett, T. Chivers, *J. Chem. Soc., Chem. Commun.* **1989**, 96−97; A. Apblett, T. Chivers, *Phorsphorus, Sulfur, Silicon Relat. Elem.* **1989**, *41*, 439−447.
[25] C. P. Warrens, J. D. Woolins, *Inorg. Synth.* **1989**, *25*, 43−47.
[26] W. L. Jolly, K. D. Maguire, *Inorg. Synth.* **1967**, *9*, 102−109.
[27] G. M. Sheldrick, SHELX-97 *Programs for Crystal Structure Analysis (Release 97−2),* Institut für Anorganische Chemie der Universität Göttingen, Germany **1997**.
[28] *Diamond-Visual Crystal Structure Information System*, Crystal Impact, Bonn, Germany.
[29] Gaussian 98, *Revision A.7*, M. J. Frisch, G. W. Trucks, H. B. Schlegel, G. E. Scuseria, M. A. Robb, J. R. Cheeseman, V. G. Zakrzewski, J. A. Montgomery, Jr., R. E. Stratmann, J. C. Burant, S. Dapprich, J. M. Millam, A. D. Daniels, K. N. Kudin, M. C. Strain, O. Farkas, J. Tomasi, V. Barone, M. Cossi, R. Cammi, B. Mennucci, C. Pomelli, C. Adamo, S. Clifford, J. Ochterski, G. A. Petersson, P. Y. Ayala, Q. Cui, K. Morokuma, D. K. Malick, A. D. Rabuck, K. Raghavachari, J. B. Foresman, J. Cioslowski, J. V. Ortiz, A. G. Baboul, B. B. Stefanov, G. Liu, A. Liashenko, P. Piskorz, I. Komaromi, R. Gomperts, R. L. Martin, D. J. Fox, T. Keith, M. A. Al-Laham, C. Y. Peng, A. Nanayakkara, C. Gonzalez, M. Challacombe, P. M. W. Gill, B. Johnson, W. Chen, M. W. Wong, J. L. Andres, C. Gonzalez, M. Head-Gordon, E. S. Replogle, and J. A. Pople, Gaussian Inc., Pittsburgh PA, **1998**.

Received February 25, 2003

